

## Plasma Directed Assembly: Process Issues, Materials and Applications

Dimitrios Kontziampasis, Athanasios Smyrnakis, Vassilios Constantoudis, Evangelos Gogolides.

N.C.S.R. "Demokritos", Aghia Paraskevi, Greece.

dkontz@imel.demokritos.gr

The modern trend in nanofabrication is the use of self or directed assembly methods to form periodic or semi-periodic patterns in the nanoscale. Block copolymer lithography and colloidal lithography are used mostly to create these patterns. Our group [1, 2] has shown that oxygen plasma can direct the formation of organized nanodots on the surface of PMMA films (Fig. 1) and then transfer the pattern to a subsequent Silicon substrate.

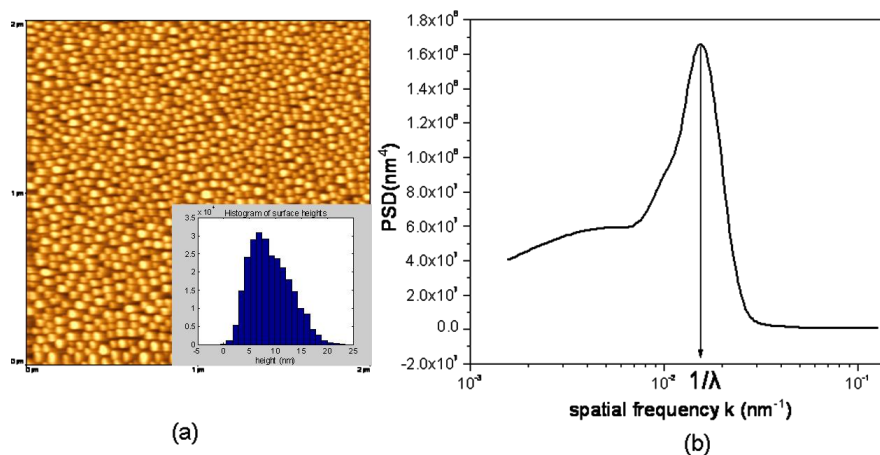
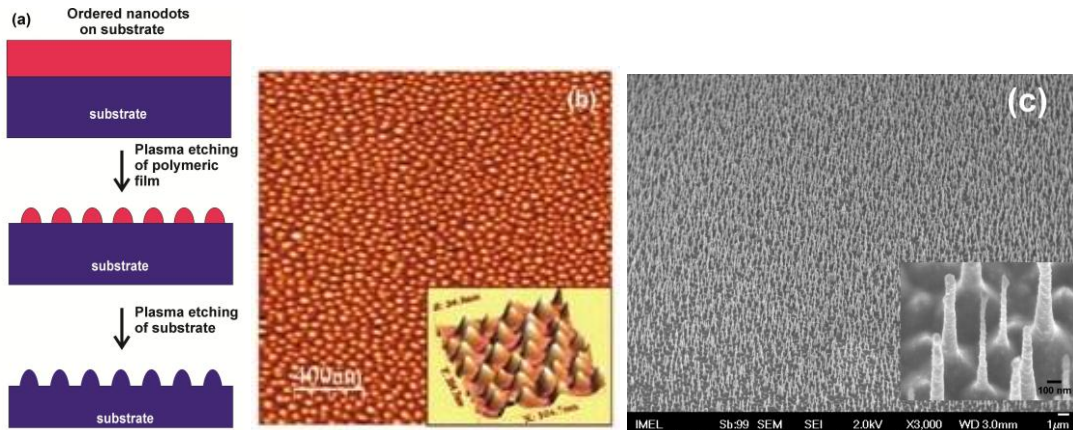


**Figure 1.** Plasma Directed Organization of Nanodots on a PMMA surface. a)  $2 \times 2 \mu\text{m}$  AFM image of an initially 750 nm thick PMMA film etched for 1min in Oxygen plasma at the following conditions (1900 W top power, 0 V bias, 0.75 Pa,  $65^\circ\text{C}$ , 1min etch, etching rate 600nm/min). Notice the formation of ordered nanodots on the surface of the film. b) PSD of the AFM image shown in (a). The peak wavenumber corresponds to a period of  $\sim 66$  nm, and the peak sharpness quantifies the extent of order formation. The histogram of surface heights is shown as an inset in Fig. 1a and reveals a distribution with skewness=0.44 and kurtosis=2.60)

With the use of a cryogenic plasma etching process we create high aspect ratio silicon nanowires or nanopillars. A schematic of the process flow is shown in Fig. 2a. Etching a polymeric film for a few tens of seconds to a few minutes, results in the formation of ordered nanodots. These nanodots may serve as a mask when they reach the substrate. For the pattern transfer to the substrate, the same plasma reactor is used by switching the discharge chemistry and conditions. Fig. 2b shows the top-down 2D morphology and embedded 3D zoomed view of periodic nanodots which develop on a PMMA film. A high density helicon plasma reactor is employed.

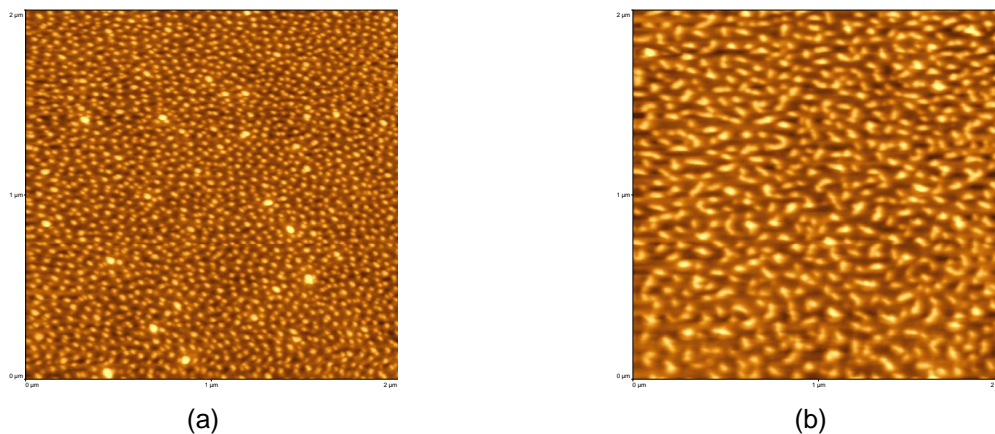
For the pattern transfer to a subsequent silicon layer and the creation of high aspect

ratio silicon nanopillars, we developed a cryogenic silicon etching process. It is a clean anisotropic process that uses a  $SF_6/O_2$  gas mixture at cryogenic temperature ( $T < -100\text{ }^\circ\text{C}$ ) which forms a  $SiO_xF_y$  passivation layer on the sidewalls that inhibits lateral etching. Having high etch selectivity to silicon over the polymeric nanodots mask, the cryogenic process was optimised in the nanoscale leading to the formation of silicon nanopillars with a diameter in the range of 40-100 nm and aspect ratio up to 20:1 (Fig. 2c). These nanopillars can find possible application for silicon solar cells or as molds for nanoimprint lithography.



**Figure 2.** (a) Process flowchart showing direct pattern transfer to the substrate using plasma etching. (b)  $2 \times 2\text{ }\mu\text{m}^2$  AFM image of a PMMA film surface after  $O_2$  plasma etching down to Si substrate (c) tilted SEM image of Si nanopillars fabricated by the cryogenic etching process (a zoomed part of the image is embedded).

In this work, we also examine the generality of the phenomenon by looking if plasma directed assembly applies in other polymers. We study Polystyrene, a thermoplastic polymer more resistant to Oxygen plasma etching than PMMA, and PET a thermoplastic polymer which is widely used in food industry (it was chosen for potential future biological applications) and compare their morphology and dot characteristics with those of PMMA, thus generalizing our previous finding of plasma directed nanodot formation on PMMA [2]. The glass transition temperature of the polymer is proposed to play a role in the size and height of the created nanodots.



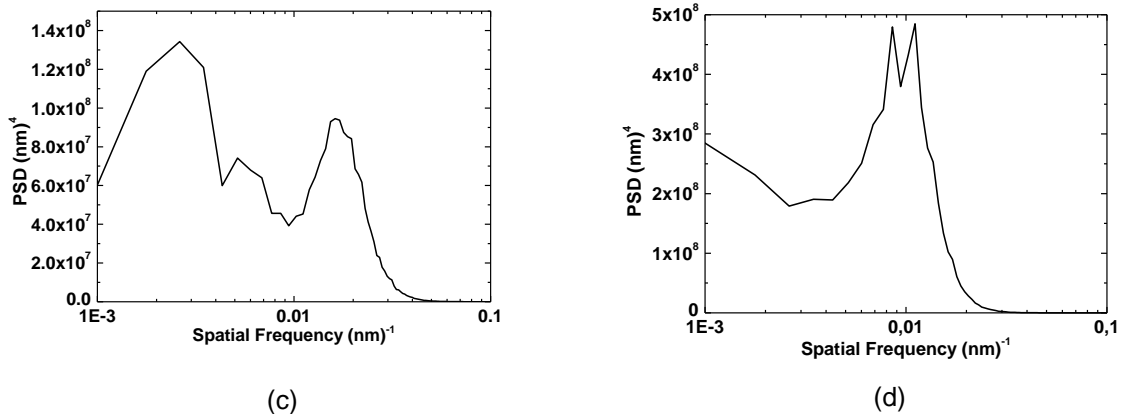


**Figure 3.** Plasma Directed Organization of Nanodots on PS and PET. (a)  $2 \times 2 \mu\text{m}^2$  AFM image of a  $\sim 1200$  nm thick PS film etched for 2 min with Oxygen plasma (conditions similar to Fig. 1, except etching rate which was  $\sim 350$  nm/min, almost half the etching rate of the PMMA polymer). (b)  $2 \times 2 \mu\text{m}^2$  AFM image of a PET plate etched for 1 min with Oxygen plasma (conditions similar to Fig. 1, except etching rate which was 680 nm/min.) (c) PSD of the 2d PS surface shown in (a). (d) PSD of the PET 2d surface shown in (b).

Processing (etching) time was also examined as to how it affects nanodot formation, along with the size of the features created and their order. We observed a second mechanism emerging after a few minutes of processing time and a transition from a small size ordered nanodots to a bigger size mounds with embedded nanodots on their surface. The emergence of this second scale topography on the etched surface affects the homogeneity of dot heights and widths resulting in much taller and wider features, which in some cases seem to form a rhomb-like network. [3]

In Figure 4, we can see the effects of the emergence of that second scale topography on vertical roughness parameters. For etching times less than 5 min, rms value remains almost unaltered with only a slight increase at 4 and 5 min. However, afterwards a dramatic change appears and rms increases very fast with a rate  $\sim 2.5$  nm/min. This crossover in rms behavior is also manifested in the time dependences of skewness and kurtosis. As one can see in Figures 4b and 4c, skewness exhibits a shift from values less than 1 to values close to 2, while kurtosis presents an abrupt increment from values around 3 to much higher ones about 6. Both changes can be attributed to the emergence of the second scale topography and the subsequent selective enhancement of the height and width of some dots since it increases the asymmetry of height distribution (upwards shift of skewness) and makes its peak steeper (increment of kurtosis).

That emergence of the second, low frequency scale and the concomitant degradation of order and homogeneity of nanodots can be also detected in the evolution of the shape of PSDs as shown in Figure 5. For times shorter than 8 mins, the PSD is characterized mainly by the presence of a peak at frequency  $f_p \sim 0.016 \text{ nm}^{-1}$  the inverse of which at  $\lambda \sim 65 \text{ nm}$  provides an estimation of the mean spacing between nearby dots. This peak widens progressively with time affecting the low frequency part of PSD, whereas at high frequencies ( $f > f_p$ ) the spectrum remains almost unaltered even for  $t = 8 \text{ min}$ . After passing the crossover time of 8 min, the low frequency part exhibits an abrupt increase (notice the log scale of PSD axis in Figure 5) and a second power law appears for  $0.002 < f < f_p$  with the simultaneous formation of a wide peak at very low

frequency. This power law quantifies in frequency terms the emergence of the second scale topography associated with low frequency fluctuations in surface morphology.

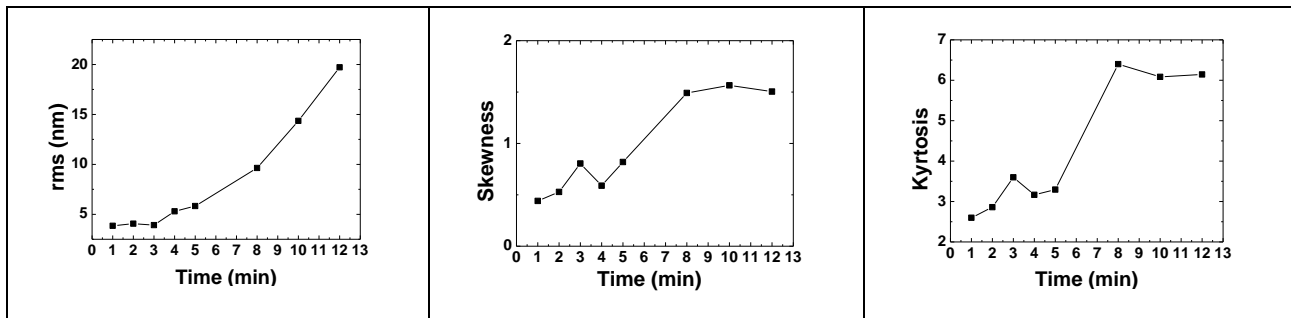


**Figure 4.** Evolution of the surface morphology metrics with oxygen plasma etching time. Vertical roughness parameters are shown versus time: rms (a), skewness (b) and kyrstosis (c).

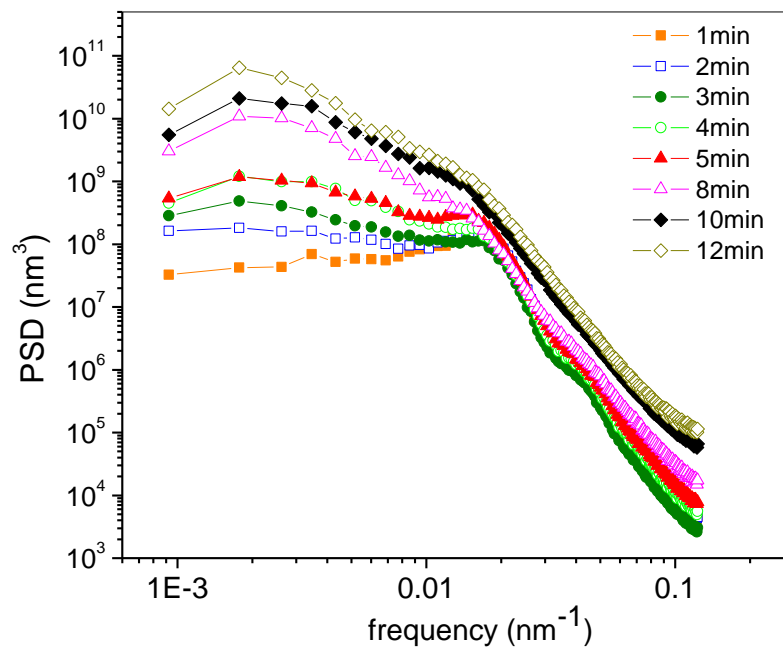


**Figure 5.** Circularly averaged Power Spectral Density (PSD) of etched surfaces versus etching time. Notice the importance of low frequency at long etching times, and the transition taking place between 5min and 8min of etching.

**References:**

[1] E. Gogolides, et. al.; PCT/GR2009/000039, WO/2009/150479.  
 [2] N. Vourdas, et. al.; Nanotechnology 21 (2010) 08530.  
 [3] D. Kontziampasis, et. al.: Plasma Proc. Polym., DOI: 10.1002/ppap.201100163